When are Non-Double-Couple Components of Seismic Moment Tensors Reliable?

Boris Rösler[1*], Seth Stein[1,2], Bruce D. Spencer[2,3]

[1]Department of Earth and Planetary Sciences, Northwestern University, Evanston IL 60208 USA

[2]Institute for Policy Research, Northwestern University, Evanston IL 60208 USA

[3]Department of Statistics and Data Science, Northwestern University, Evanston IL 60208 USA

*Corresponding author: boris@earth.northwestern.edu

Submitted to Seismica

Abstract

Non-double-couple (NDC) components of seismic moment tensors (MTs) may indicate complex source processes differing from slip on a fault for earthquakes in specific geologic environments, reflect the combined effect of double-couple sources on multiple faults with different geometries, or be artifacts of the MT inversion without geologic meaning. Hence there has been considerable discussion in the literature as to how to assess when NDC components are real rather than artifacts. Several authors have proposed varying thresholds above which NDC components are likely to be real. We explore this question using a much larger global dataset and earthquake magnitude range by comparing the moment tensors of earthquakes in three global catalogs, which use different inversion procedures. The NDC components of MTs for 5000 earthquakes with $4.4 \leqq Mw \leqq 8.6$ common to the catalogs of the Global CMT Project, German Research Centre for Geosciences (GFZ), and U.S. Geological Survey (USGS) are only weakly correlated between catalogs, suggesting that they are largely artifacts of the inversion. A monotonic decrease in the NDC component's standard deviation with magnitude indicates increased reliability of the NDC components for larger earthquakes. The standard deviation with size of the NDC components begins to decrease for NDC components exceeding 60%, suggesting that the threshold for NDC components representing real source processes is much larger than previously proposed. This decrease appears to be partially a consequence of the definition of the NDC components: Randomly generated NDC components with the same mean and standard deviation as in the three MT catalogs show that large NDC components are more likely to exceed values that are excluded by their definition. The remaining NDC components have a smaller standard deviation, reproducing the decrease in standard deviation in the three MT catalogs for the largest NDC components. However, this decrease is smaller than that observed. Thus NDC components of large earthquakes and NDC components that exceed 60% are likely to represent real source processes. The variation of standard deviation between earthquakes with different faulting types is a consequence of the variation of the size of the NDC components between faulting types.

Introduction

Moment tensors provide a general description of seismic sources which may include components that differ from slip on planar faults. Following the deployment of large digital seismic networks and the automatic derivation of moment tensors (MTs) after an earthquake, it was observed that many MTs had non-double-couple (NDC) components (*Frohlich*, 1994) whose geologic meaning has been debated (*Sipkin*, 1986; *Miller et al.*, 1998).

Because the isotropic components of MTs are generally small (*Kawakatsu*, 1991; *Okal et al.*, 2018), catalogs usually constrain the isotropic component during the inversion to be zero and report only deviatoric MTs (*Dziewonski and Woodhouse*, 1983; *Ekström et al.*, 2012). Constraining the isotropic component also reduces the appearance of spurious compensated linear vector dipole (CLVD) components (*Vavryčuk*, 2001). CLVD components describe three force dipoles with one twice the magnitude of the others, yielding no volume change (*Knopoff and Randall*, 1970). Because CLVD components are the only possible NDC components in deviatoric MT catalogs, we use the terms interchangeably.

Some earthquakes in specific geologic environments, notably volcanic ones, have NDC components that have been interpreted to represent real source processes (*Kanamori and Given*, 1982; *Ross et al.*, 1996; *Nettles and Ekström*, 1998). Other NDC components reflect near-simultaneous rupture on nearby faults with different geometry (e.g. *Hayes et al.,* 2010; *Hamling et al.*, 2017; *Scognamiglio et al.*, 2018; *Yang et al.*, 2021; *Ruhl et al.*, 2021) or a rupture with changes in geometry (*Wald and Heaton*, 1994; *Pang et al.*, 2020). However, NDC components can also be artifacts of the MT inversion without geologic meaning (*Ammon et al.*, 1994; *Chapman*, 2013).

Determining the origin of NDC components of earthquakes reported by MT inversions without additional information about the geologic setting of the earthquake is challenging. *Rösler and Stein* (2022) examined a large moment tensor dataset to assess how NDC components vary between earthquakes. Their general consistency with magnitude and faulting type and hence geologic environment suggests that most NDC components are artifacts of the inversion procedures used in compiling different catalogs.

However, several studies argue that there exists a threshold above which NDC components represent real source processes. *Vavryčuk's* (2002) study of M<3 events in Bohemia placed this threshold between 20 and 40%. *Stierle et al*.'s (2014) analysis of M<4.1 aftershocks of the 1999 Izmit earthquake found that spurious NDC components can reach 15%, and *Adamová and Šílený's* (2010) modeling study determined that spurious components can exceed 20%. In this study, we consider earthquakes worldwide with 4.4≦Mw≦8.6 and use the differences between NDCs in different catalogs to assess their reliability and thus the issue of a possible threshold.

Methodology

The Global CMT (GCMT) Project (*Ekström et al.*, 2012), German Research Centre for Geosciences (GFZ), and U.S. Geological Survey (USGS) catalogs provide deviatoric moment tensors for a global distribution of earthquakes. We compile a dataset of 5000 earthquakes common to all three catalogs from July 2011 to December 2021 (Fig. 1), and identify MTs describing the same event by similar source times (± 60s), locations (difference less than 1°), and magnitudes (Mw ± 0.5). We use the USGS catalog's definition of the scalar moment as the Euclidian norm of the moment tensor (*Silver and Jordan*, 1982)

$$M_0 = \sqrt{\frac{1}{2}\sum_{i=1}^{3}\sum_{j=i}^{3} M_{ij}^2},$$

which is equivalent to the square root of the sums of the squares of the eigenvalues $\lambda_i^{'}$. This definition differs from that in the GCMT catalog, which uses the scalar moment of the best-fitting double-couple. From the scalar moment, we calculate the earthquake's moment magnitude

$$Mw = \frac{2}{3}(log_{10}M_0 - 9.1).$$

For each earthquake, the NDC component in each catalog is obtained as twice the ratio of the smallest and absolutely largest eigenvalues of the MT,

$$2\epsilon = \frac{2\lambda_3'}{max(|\lambda_1'|,|\lambda_2'|)},$$

where $\lambda_1 > \lambda_3 > \lambda_2$. The mean NDC component for an earthquake is calculated as the mean of the NDC components in the three catalogs,

$$2\overline{\epsilon} = \frac{2}{3}(\epsilon_1 + \epsilon_2 + \epsilon_3),$$

and the NDC's standard deviation is

$$\sigma = \sqrt{\frac{4}{3}\sum_{i=1}^{3}(\epsilon_i - \overline{\epsilon})^2}.$$

To classify earthquakes by faulting type, we calculate the plunge of the P-, N-, and T-axes from the eigenvectors of the moment tensors (*Frohlich*, 1992). An earthquake is considered a normal faulting earthquake if the plunge of its P-axis satisfies $\sin^2 \delta_P \geqq 2/3$ ($\delta_P \geqq 54.75°$), strike-slip if its N-axis plunge exceeds 54.75°, and a thrust fault if its T-axis plunge exceeds 54.75° (*Saloor and Okal*, 2018). If the plunge of none of the axes exceeds the threshold, we consider an earthquake to have oblique faulting.

Results

The NDC components in our dataset have a similar distribution with magnitude in all three catalogs (Fig. 2). The decrease with magnitude has been observed by *Rösler and Stein* (2022), who, using a large dataset compiled from multiple global and regional MT catalogs, found an average NDC component of 23.2% that varies only slightly with magnitude.

However, the values of the NDC components for earthquakes in the three catalogs are only weakly correlated between catalogs (Fig. 3), consistent with findings by Frohlich and Davis (1999). Hence the standard deviation of the NDC components for each earthquake in the catalogs is a measure of the NDC component's reproducibility and can be used to assess the reliability of its determination. Figure 4a shows that the standard deviation among the three catalogs decreases significantly with the magnitude of an earthquake, suggesting a more consistent determination of NDC components for larger earthquakes.

Rösler et al. (2021) found that the source processes of large earthquakes are more reliably determined, which is consistent with our dataset. Because the size of the NDC components vary only slightly for earthquakes of different magnitudes (Fig. 2), we attribute the decrease in their standard deviation to the magnitude of the earthquake, indicating that NDC components of large earthquakes are more reliable than the ones of small earthquakes.

Similarly, figure 4b shows a decrease of the standard deviation for NDC components larger than 60%. This observation may support the existence of a threshold above which NDC components represent real source processes. However, a complexity arises for large NDC components because, by definition, these cannot exceed 100%. When the mean of the NDC components from the three catalogs is large in absolute value, the individual measurements tend to be closer than average. An extreme example illustrates this point. If the NDC component has an average (among the three catalogs) of 99%, the largest variation that could occur among the three individual values is for 100%, 100%, and 97%, and for these values the standard deviation is below 1.75%. A related phenomenon is found in the binomial distribution in statistics, where the standard deviation decreases as the probability parameter increases beyond 50%.

To explore the possible impact of this effect, we conducted a simulation in which we randomly generated NDC components with the same mean as the observed triple from the three catalogs and the same standard deviation as the entire dataset. To do this, we first generated three sets of 5000 random values x, y, and z independently from a Gaussian distribution with zero mean and the standard deviation as in our dataset (σ = 13.3%). We then set $X_i = m_i + ax_i – by_i – bz_i$, $Y_i = m_i - bx_i + ay_i – bz_i$, and $Z_i = m_i - bx_i – by_i + az_i$ for all i= 1, 2, …, 5000 with $a = (2/3)^{1/2}$, $b = (1/6)^{1/2}$, and m_i being the mean NDC component for each earthquake among the three catalogs. The resulting X, Y, and Z each have mean m, standard deviation σ, and equal correlations so that the variance of their sum equals zero, i.e., $V(X + Y + Z) = 0$. The triples provide a set of three catalogs whose NDC components have the same mean and standard deviation as the observed datasets.

Figure 5a shows that the standard deviation of these randomly generated NDC components does not vary with the size of the NDC components. However, this dataset contains values for which individual NDC components exceed $2|\varepsilon| > 100\%$, which violates the definition of NDC components. Recall that the NDC component depends on the size of the smallest eigenvalue λ_3. If λ_3 becomes larger in absolute value than one of the other eigenvalues λ_1 or λ_2 where $2|\varepsilon| = 100\%$, the eigenvalues switch order and the NDC component decreases in size and approaches a DC source again.

Discarding NDC components for which individual values exceed the ceiling of 100% truncates the random dataset to values which are physically possible. Because individual NDC components of > 100% are more likely for large mean NDC components, the bin of largest NDC components with $2|\varepsilon| > 80\%$ is expected to be most affected by this truncation. Figure 5b shows that this process eliminates the triples of random NDC components with the largest standard deviation, leading to a decrease in standard deviation for the bin of largest NDC components while leaving other bins practically unchanged. This decrease is similar to that in the observed dataset (Fig. 4b). Repeating this experiment 10,000 times results in an average decrease in standard deviation of 3.3% for this bin (Fig. 5c), which is smaller than in the observed dataset. Instead of discarding NDC components larger than 100%, it is also possible to include them as smaller NDC components in this experiment. This can be done in different ways: If we limit the largest NDC components to 100%, we increase the smallest by the amount the largest NDC component exceeded 100% to preserve the mean of each triple. Repeating this experiment 10,000 times results in an average decrease in standard deviation of 2.0% in the largest size bin after modification of the NDC components exceeding 100%. Reducing the largest NDC components to values below 100% corresponding by the amount those NDC components exceeded 100% is equivalent to the decrease in NDC component when the smallest eigenvalue λ_3 continues to increase and switches order with another eigenvalue. To preserve the mean of each triple of NDC components in this case, we increase the smallest NDC component by twice the amount by which the largest NDC component exceeded 100%. Repeating this experiment 10,000 times results in a decrease in standard deviation of 3.1% for the bin of largest NDC components, comparable in size to discarding triples where individual values exceed values allowed by their definition, which results in a decrease of 3.3% in standard deviation. The standard deviation can be minimized when also modifying the intermediate NDC component: Assuming $|X_i| \geqq |Y_i| \geqq |Z_i|$, we calculate $d = \mathrm{sgn}(X_i)(|X_i| - 100\%)$ and replace X_i by $X_i - 2d$, Y_i by $Y_i + gd$, and Z_i by $Z_i + (2 - g)d$, where $g = 1 - (Y_i - Z_i)/(2d)$. If the new value of Y_i exceeds 100%, we reduce it to 100% and increase X_i accordingly. In this case, the standard deviation decreases by 4.0% after 10,000 repetitions in the largest NDC components bin.

Therefore, this ceiling effect produces a distribution of standard deviation with size of the NDC component similar to that in the MT catalogs, but with a smaller decrease in the bin of largest NDC components. The observed dataset shows a standard deviation of 6.0% for NDC components larger than 80%, 7.3% smaller than the standard deviation for the complete dataset of 13.3%. Moreover, the ceiling effect does not reproduce the observed decrease in standard deviation for the bin of second largest NDC components between 60-80%, where the random NDC components only show an insignificant change. We hence conclude that the largest NDC components are, on average, more reliably determined. However, the threshold above which NDC components can be considered reliable, based on the significant decrease in standard deviation among NDC components in different catalogs, lies at around 60%. This value is much larger than proposed in earlier studies.

Rösler and Stein (2022) noticed that the size of NDC components varies with faulting type. Consistent with their observation, thrust-faulting earthquakes have the smallest NDC components on average of all different faulting types in our dataset (Fig. 6a). Their standard deviation between catalogs varies as well, with thrust-faulting earthquakes having the smallest (Fig. 6b). This is expected because the standard deviation of a Gaussian distribution with zero mean determines the mean of the absolute values. Therefore, it is unsurprising that the standard deviation of the different faulting types reflects the average size of NDC components, which suggests that the reliability between NDC components does not vary between faulting types.

Discussion and Conclusions

Global MT catalogs use different inversion procedures to derive solutions for the source processes of earthquakes. These procedures may vary in the stations used for the inversion, the individual weights given to the stations, the frequency of seismic waves, the processing of waveforms, and the inversion algorithm. The standard deviation between the NDC components in different catalogs is a measure of the difference between them and hence their reproducibility. In this study, we use a dataset of 5000 MTs of earthquakes common to the catalogs of the Global CMT Project, the GFZ, and the USGS to assess the reliability of NDC components of seismic MTs.

The standard deviation of observed NDC components decreases for NDC components that are larger than 60%. Generating random NDC components with the same mean and standard deviation as the observed dataset shows that the decrease in standard deviation for the largest NDC components can be only partially explained by the constraint that NDC components must satisfy $2|\varepsilon| < 100\%$ rather than a higher reliability of large NDC components. We therefore conclude that the largest NDC components are generally more reliably determined, and the threshold above which NDC components in global MT catalogs likely represent real source processes is about three times larger the observed average of NDC components of around 20%. Hence our sense is that an NDC component greater than 60% is likely to reflect a real source process, although different moment tensor inversions may yield different results. Smaller NDC components are likely to be artifacts, and thus need further investigation before they can be considered real.

The standard deviation between NDC components in different catalogs decreases monotonically with the magnitude of an earthquake (Fig. 4a). Figures 7a and b show that the randomly generated NDC components exceeding 100% are distributed arbitrarily among the magnitude bins. They are most likely to fall into the magnitude bins with the most earthquakes and hence the smallest magnitude bins. In contrast to the distribution with size, the distribution of random NDC components with magnitude does not create a ceiling effect. Additionally, large earthquakes have, on average, smaller NDC components (Fig. 2). As a consequence, the largest magnitude bin is, in most cases, unaffected by NDC components exceeding a size of 100% and deleting them from the dataset or modifying them has no influence on the standard deviation in any magnitude bin. Repeating the experiment 10,000 times shows no difference in standard deviation in the largest magnitude bin. Therefore, in the absence of ceiling constraints, the observed decrease in standard deviation for NDC components of large earthquakes reflects the magnitude of an earthquake. As a consequence, the better agreement between catalogs suggests a higher reliability of NDC components of large earthquakes.

The variation of the NDC's standard deviation between faulting types does not reflect a variation in reliability, and is a consequence of the varying size of NDC components between faulting types. Therefore, only the variation of NDC components with earthquake magnitude appears to indicate at a variation in reliability of the NDC component.

Data and Resources

The moment tensors used in this study were compiled from publicly available data sets. GCMT solutions are *from https://www.globalcmt.org* (last accessed June 2022). The USGS and GFZ catalogs were downloaded using the Python package ObsPy and its International Federation of Digital Seismograph Networks webservice client (June 2022). A list of the earthquakes used in this study including their moment tensors in different catalogs is available as an electronic supplement.

Acknowledgements

We thank Emile Okal and Craig Bina for helpful discussions.

References

Adamová, P., and Šílený, J. (2010). *Non-double-couple earthquake mechanism as an artifact of the point-source approach applied to a finite-extent focus,* Bull. Seismol. Soc. Am., **100**, no. 2, 447-457.

Ammon, C. J., Lay, T., Velasco, A. A., and Vidale, J. E. (1994). *Routine estimation of earthquake source complexity: The 18 October 1992 Colombian earthquake*, Bull. Seismol. Soc. Am., **84**, no. 4, 1266-1271.

Chapman, M. C. (2013). *On the rupture process of the 23 August 2011 Virginia earthquake*, Bull. Seismol. Soc. Am., **103**, no. 2A, 613-628.

Dziewonski A. M., and Woodhouse, J. (1983). *An experiment in systematic study of global seismicity: centroid-moment tensor solutions for 201 moderate and large earthquakes of 1981*, J. Geophys. Res., **88**, no. B4, 3247-3271.

Ekström, G., Nettles, M., and Dziewoński, A. M. (2012). The global CMT project 2004–2010: Centroid-moment tensors for 13,017 earthquakes, *Phys. Earth. Planet In.*, **200**, 1-9.

Frohlich, C. (1992). *Triangle diagrams: ternary graphs to display similarity and diversity of earthquake focal mechanisms*, Phys. Earth Planet. In., **75**, nos. 1/3, 193–198.

Frohlich, C. (1994). *Earthquakes with non-double-couple mechanisms*, Science, **264**, no. 5160, 804–809.

Frohlich, C., and S. D. Davis (1999). *How well constrained are well-constrained T, B, and P axes in moment tensor catalogs?*, J. Geophys. Res. **104**, no. B3, 4901–4910.

Hamling, I. J., Hreinsdóttir, S., Clark, K., Elliott, J., Liang, C., Fielding, E., ..., and d'Anastasio, E. (2017). *Complex multifault rupture during the 2016 Mw 7.8 Kaikōura earthquake, New Zealand*, Science, **356**, no. 6334.

Hayes, G. P., Briggs, R. W., Sladen, A., Fielding, E. J., Prentice, C., Hudnut, K., ..., and Ito, T. (2010). *Complex rupture during the 12 January 2010 Haiti earthquake*, Nat. Geosci., **3**, no. 11, 800-805.

Kanamori, H., and Given, J. W. (1982). *Analysis of long-period seismic waves excited by the May 18, 1980, eruption of Mount St. Helens—A terrestrial monopole?*, J. Geophys. Res. Solid Earth, **87**, no. B7, 5422-5432.

Kawakatsu, H. (1991). *Insignificant isotropic component in the moment tensor of deep earthquakes*. Nature, **351**(6321), 50-53.

Knopoff, L., and M. J. Randall (1970). *The compensated linear-vector dipole: A possible mechanism for deep earthquakes*, J. Geophys. Res., **75**, no. 26, 4957–4963.

Miller, A. D., G. R. Foulger, & B. R. Julian (1998). *Non-double- couple earthquakes 2. Observations*, Rev. Geophys., **36**, no. 4, 551–568.

Nettles, M., and Ekström, G. (1998). *Faulting mechanism of anomalous earthquakes near Bárdarbunga Volcano, Iceland*, J. Geophys. Res. Solid Earth, **103**, no. B8, 17973-17983.

Okal, E. A., Saloor, N., Kirby, S. H., and Nettles, M. (2018). *An implosive component to the source of the deep Sea of Okhotsk earthquake of 24 May 2013: Evidence from radial modes and CMT inversion*, Phys. Earth Planet. In., *281*, 68-78.

Pang, G., Koper, K. D., Mesimeri, M., Pankow, K. L., Baker, B., Farrell, J., ..., and DuRoss, C. (2020). *Seismic analysis of the 2020 Magna, Utah, earthquake sequence: Evidence for a listric Wasatch fault*, Geophys. Res. Lett., **47,** no. 18

Rösler, B., Stein, S., and Spencer, B.D. (2021). *Uncertainties in Seismic Moment Tensors Inferred from Differences Between Global Catalogs*, Seismol. Res. Lett., **92** no. 6, 3698–3711, doi: 10.1785/0220210066.

Rösler, B., and Stein, S. (2022). *Consistency of Non-Double-Couple Components of Seismic Moment Tensors with Earthquake Magnitude and Mechanism*, Seismic. Res. Lett., **93**, no. 3, 1510-1523.

Ross, A., Foulger, G. R., & Julian, B. R. (1999). *Source processes of industrially-induced earthquakes at The Geysers geothermal area, California*. Geophysics, **64**(6), 1877-1889.

Ruhl, C. J., Morton, E. A., Bormann, J. M., Hatch-Ibarra, R., Ichinose, G., and Smith, K. D. (2021). *Complex Fault Geometry of the 2020 Mww 6.5 Monte Cristo Range, Nevada, Earthquake Sequence,* Seismol. Res. Lett., **92**, no. 3, 1876-1890.

Saloor, N., and E. A. Okal (2018). *Extension of the energy-to-moment parameter θ to intermediate and deep earthquakes*, Phys. Earth Planet. In., **274**, 37–48.

Silver, P. G., and Jordan, T. H. (1982), *Optimal estimation of scalar seismic moment*, Geophys. J. Int., **70,** no. 3, 755-787.

Scognamiglio, L., Tinti, E., Casarotti, E., Pucci, S., Villani, F., Cocco, M., ... & Dreger, D. (2018). *Complex fault geometry and rupture dynamics of the MW 6.5, 30 October 2016, Central Italy earthquake*. Journal of Geophysical Research: Solid Earth, **123**(4), 2943-2964.

Sipkin, S. A. (1986). Interpretation of non-double-couple earthquake mechanisms derived from moment tensor inversion, *J. Geophys. Res. Solid Earth*, **91**, no. B1, 531-547.

Stierle, E., Bohnhoff, M., & Vavryčuk, V. (2014). *Resolution of non-double-couple components in the seismic moment tensor using regional networks—II: application to aftershocks of the 1999 M w 7.4 Izmit earthquake*. *J. Geophys. Res. Solid Earth*, *196*(3), 1878-1888.

Vavryčuk, V. (2001). *Inversion for parameters of tensile earthquakes*. *J. Geophys. Res. Solid Earth*, **106**(B8), 16339-16355.

Vavryčuk, V. (2002). *Non-double-couple earthquakes of 1997 January in West Bohemia, Czech Republic: evidence of tensile faulting*. Geophys. J. Int., **149**(2), 364-373.

Wald, D. J., and Heaton, T. H. (1994). *Spatial and temporal distribution of slip for the 1992 Landers, California*, earthquake, Bull. Seismol. Soc. Am., **84,** no. 3, 668-691.

Yang, J., Zhu, H., Lay, T., Niu, Y., Ye, L., Lu, Z., ... and Li, Z. (2021). *Multi-fault opposing-dip strike-slip and normal-fault rupture during the 2020 Mw 6.5 Stanley, Idaho earthquake*. Geophys. Res. Lett., **48**, no. 10.

Authors

Boris Rösler

Northwestern University, Department of Earth and Planetary Sciences, 2145 Sheridan Road, Evanston, IL 60208, boris@earth.northwestern.edu

Seth Stein

Northwestern University, Department of Earth and Planetary Sciences and Institute for Policy Research, 2145 Sheridan Road, Evanston, IL 60208, s-stein@northwestern.edu

Bruce D. Spencer

Northwestern University, Department of Statistics and Data Science, 2006 Sheridan Road, Evanston, IL 60208, bspencer@northwestern.edu

List of Figure Captions

1. Location and focal mechanisms of the 5000 earthquakes used in this study. The earthquakes occurred between July 2011 and December 2021. Shown are the focal mechanisms in the Global CMT Project catalog.

2. Distribution of NDC components with magnitude in the three MT catalogs. Shown are the mean NDC component and the 95% confidence interval, calculated as twice the standard deviation of the mean. The distribution in all catalogs is similar, with NDC components decreasing with magnitude.

3. Correlation of NDC components between each two of the three catalogs. Despite slight variations, the correlation between NDC components in different catalogs is weak, hinting at large uncertainties in their determination.

4. Standard deviation among NDC components in different catalogs with a) magnitude of the earthquake and b) size of the NDC component, and 95% confidence intervals for mean standard deviations. The standard deviation, a measure of their reproducibility, decreases significantly with magnitude, suggesting more reliable determination of NDC components for large earthquakes. The standard deviation decreases similarly for the largest NDC components.

5. a) Standard deviation of randomly generated NDC components from a Gaussian distribution with the same mean and standard deviation as the MTs in our dataset. The standard deviation is constant over the range of sizes of NDC components. b) Some randomly generated NDC components exceed 100% (marked in red). Discarding these values decreases the standard deviation for the largest NDC component bin ($2|\varepsilon| > 80\%$). c) Repeating this experiment 10,000 times yields a 3.3% average decrease, smaller than for the observed NDC components.

6. a) Mean NDC components of earthquakes with different faulting types in the three catalogs and their mean for each faulting type. The 95% confidence interval is too small to be shown in the plot. b) Standard deviation of NDC components between catalogs for earthquakes with different faulting types. The standard deviation reflects the average size of the NDC components because the standard deviation of a Gaussian distribution with zero mean determines the mean of the absolute values. Therefore, the variation in standard deviation between faulting types does not reflect varying reliability.

7. a) Standard deviation of the randomly generated NDC components in figure 3 with magnitude. The standard deviation is constant over all magnitudes. b) Discarding values for which individual NDC components exceed $2|\varepsilon| > 100\%$ does not have influence on the standard deviation in any magnitude bin. c) Repeating this experiment 10,000 times shows that deleting large NDC components does not affect the standard deviation in the largest magnitude bin. Therefore, randomly generated NDC components cannot reproduce the observed decrease in standard deviation for the largest earthquakes, which suggests an increased reliability of NDC components for large earthquakes.

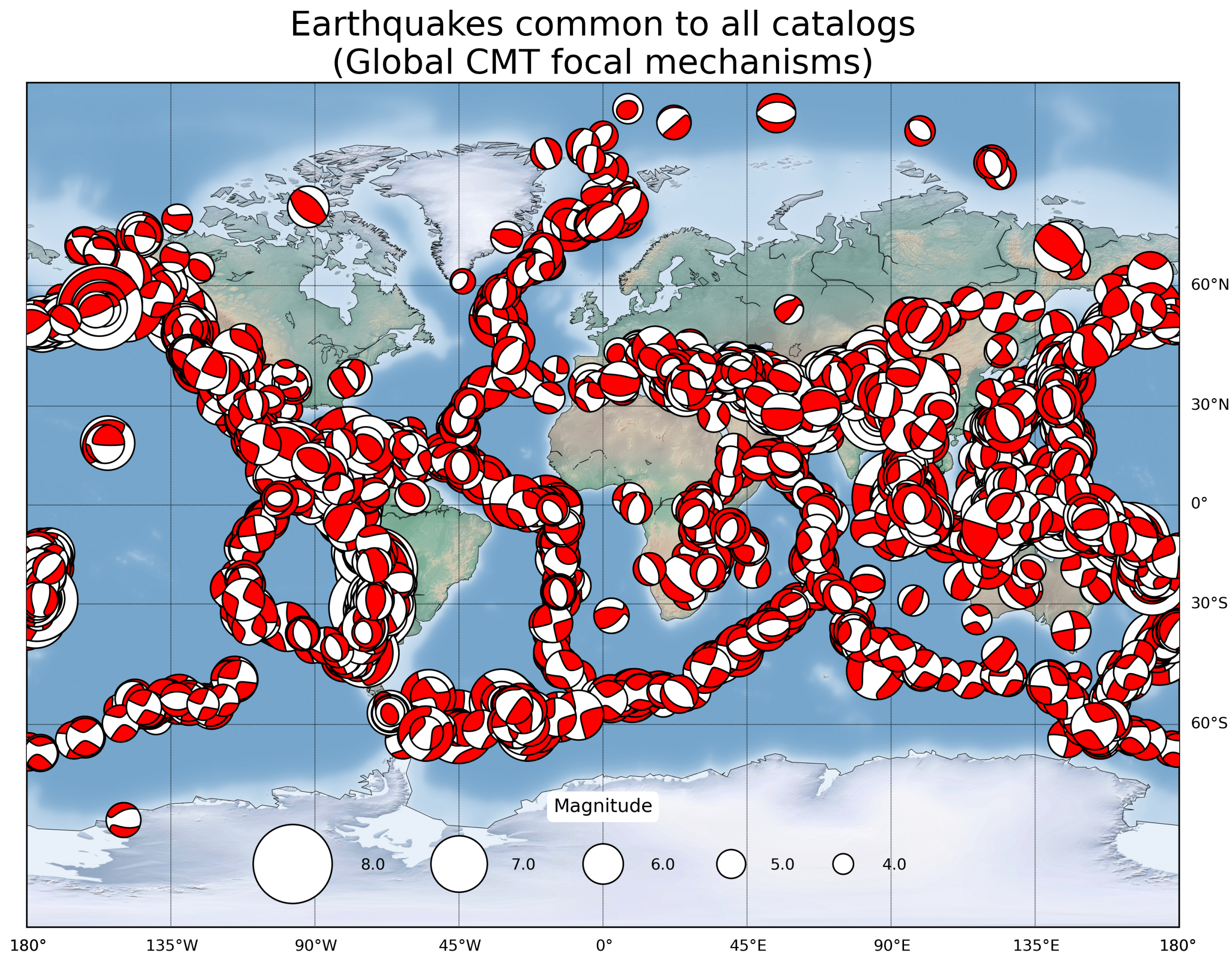

Figures

1. Location and focal mechanisms of the 5000 earthquakes used in this study. The earthquakes occurred between July 2011 and December 2021. Shown are the focal mechanisms in the Global CMT Project catalog.

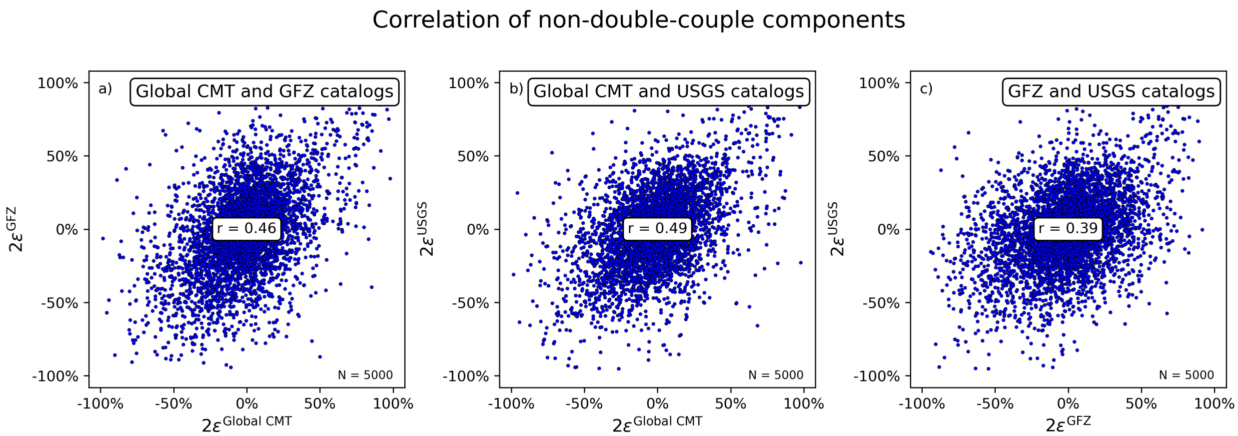

2. Distribution of NDC components with magnitude in the three MT catalogs. Shown are the mean NDC component and the 95% confidence interval, calculated as twice the standard deviation of the mean. The distribution in all catalogs is similar, with NDC components decreasing with magnitude.Correlation of NDC components between each two of the three catalogs. Despite slight variations, the correlation between NDC components in different catalogs is weak, hinting at large uncertainties in their determination.

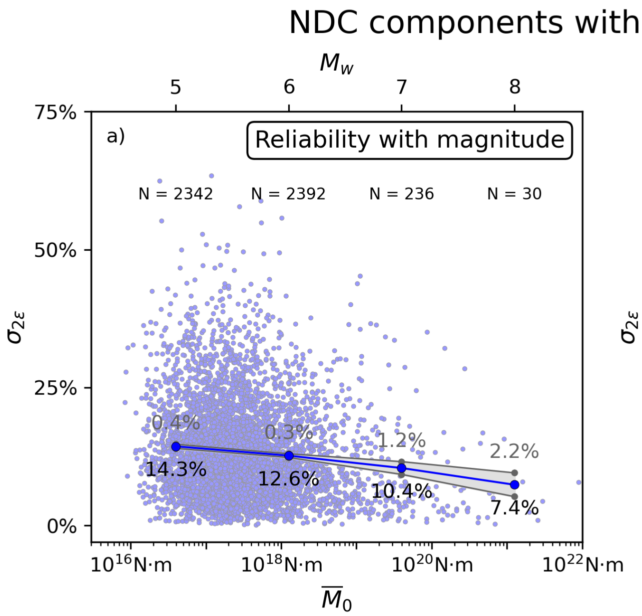

3. Standard deviation among NDC components in different catalogs with a) magnitude of the earthquake and b) size of the NDC component, and 95% confidence intervals for mean standard deviations. The standard deviation, a measure of their reproducibility, decreases significantly with magnitude, suggesting more reliable determination of NDC components for large earthquakes. The standard deviation decreases similarly for the largest NDC components.

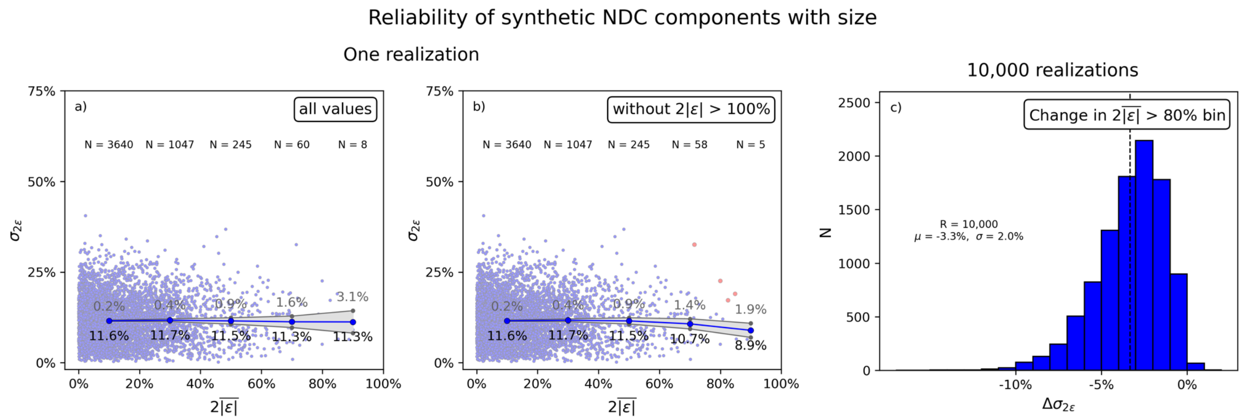

4. a) Standard deviation of randomly generated NDC components from a Gaussian distribution with the same mean and standard deviation as the MTs in our dataset. The standard deviation is constant over the range of sizes of NDC components. b) Some randomly generated NDC components exceed 100% (marked in red). Discarding these values decreases the standard deviation for the largest NDC component bin (2|ε| >80%). c) Repeating this experiment 10,000 times yields a 3.3% average decrease, smaller than for the observed NDC components.

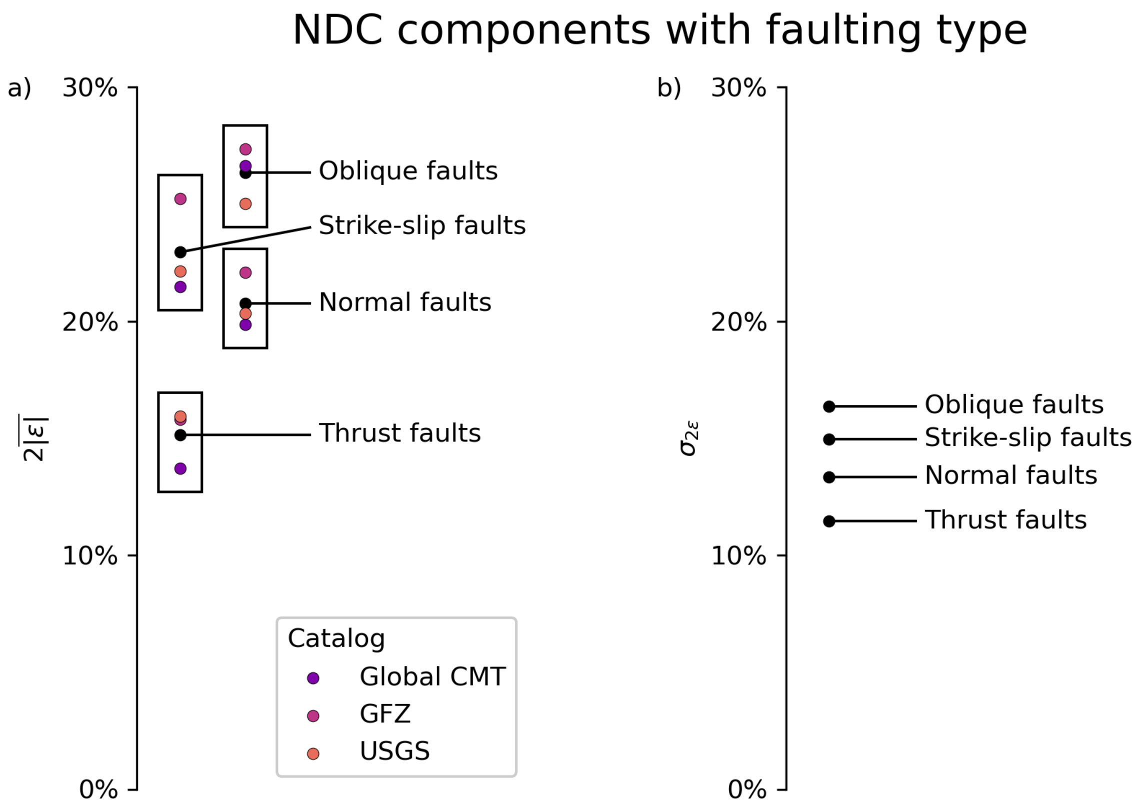

5. a) Mean NDC components of earthquakes with different faulting types in the three catalogs and their mean for each faulting type. The 95% confidence interval is too small to be shown in the plot. b) Standard deviation of NDC components between catalogs for earthquakes with different faulting types. The standard deviation reflects the average size of the NDC components because the standard deviation of a Gaussian distribution with zero mean determines the mean of the absolute values. Therefore, the variation in standard deviation between faulting types does not reflect varying reliability.

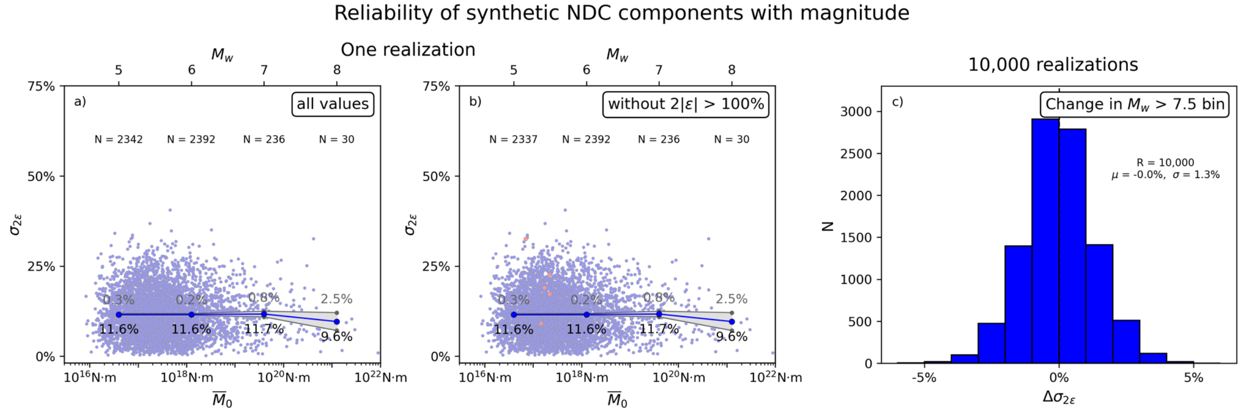

6. a) Standard deviation of the randomly generated NDC components in figure 3 with magnitude. The standard deviation is constant over all magnitudes. b) Discarding values for which individual NDC components exceed 2|ε| > 100% does not have influence on the standard deviation in any magnitude bin. c) Repeating this experiment 10,000 times shows that deleting large NDC components does not affect the standard deviation in the largest magnitude bin. Therefore, randomly generated NDC components cannot reproduce the observed decrease in standard deviation for the largest earthquakes, which suggests an increased reliability of NDC components for large earthquakes.